Supplementary Material for

Separating daily 1 km $PM_{2.5}$ inorganic chemical composition in China since 2000 via deep learning integrating ground, satellite, and model data

Jing Wei[1*], Zhanqing Li[1*], Xi Chen[2*], Chi Li[3], Yele Sun[4], Jun Wang[5], Alexei Lyapustin[6], Guy Pierre Brasseur[7,8], Mengjiao Jiang[7,9], Lin Sun[10], Tao Wang[11], Chang Hoon Jung[12], Bing Qiu[13], Cuilan Fang[14], Xuhui Liu[15], Jinrui Hao[15], Yan Wang[16], Ming Zhan[17], Xiaohong Song[18], Yuewei Liu[19]

1. Department of Atmospheric and Oceanic Science, Earth System Science Interdisciplinary Center, University of Maryland, College Park, Maryland 20742, USA
2. National Institute of Environmental Health, Chinese Center for Disease Control and Prevention, Beijing 100050, China
3. Department of Energy, Environmental and Chemical Engineering, Washington University in St. Louis, St. Louis, Missouri 63130, USA
4. State Key Laboratory of Atmospheric Boundary Physics and Atmospheric Chemistry Institute of Atmospheric Physics, Chinese Academy of Sciences, Beijing 100029, China
5. Department of Chemical and Biochemical Engineering, Iowa Technology Institute, University of Iowa, Iowa 52242, United States
6. Laboratory for Atmospheres, NASA Goddard Space Flight Center, Greenbelt, Maryland 20771, USA
7. Max Planck Institute for Meteorology, Hamburg 20146, Germany
8. National Center for Atmospheric Research, Boulder, Colorado 80307, USA.
9. School of Atmospheric Sciences, Chengdu University of Information Technology, Chengdu 610225, China
10. College of Geodesy and Geomatics, Shandong University of Science and Technology, Qingdao 266590, China
11. Department of Civil and Environmental Engineering, The Hong Kong Polytechnic University, Hong Kong 999077, China
12. Department of Health Management, Kyungin Women's University, Incheon 21041, Korea
13. Civil Aviation Medical Center, Civil Aviation Administration of China, Beijing 100123, China
14. Jiulongpo Center for Disease Control and Prevention, Chongqing 400039, China
15. Taiyuan Center for Disease Control and Prevention, Taiyuan 030015, China
16. Harbin Center for Disease Control and Prevention, Harbin 150010, China
17. Pudong Center for Disease Control and Prevention, Shanghai 200120, China
18. Shimadzu (China) Co., LTD., Beijing 100020, China
19. Department of Epidemiology, School of Public Health, Sun Yat-sen University, Guangzhou, Guangdong 510080, China

*Corresponding authors:
zli@atmos.umd.edu; chenxi@nieh.chinacdc.cn; weijing_rs@163.com

Contents of this file

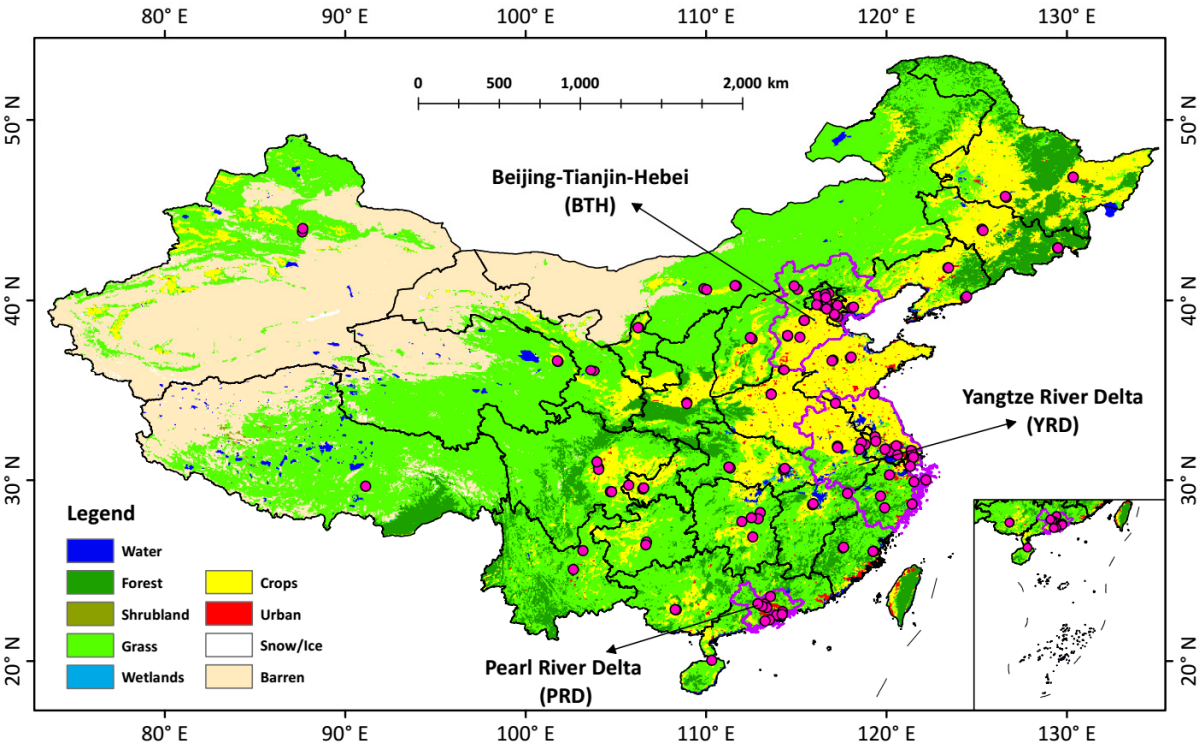

Figure S1. Geographical locations of ground-based stations of $PM_{2.5}$ composition (marked as pink dots) from the Chinese Center for Disease Control and Prevention, and background colored map indicates the land-use type. Purple delineates the Beijing–Tianjin–Hebei (BTH) region, the Yangtze River Delta (YRD), and the Pearl River Delta (PRD).

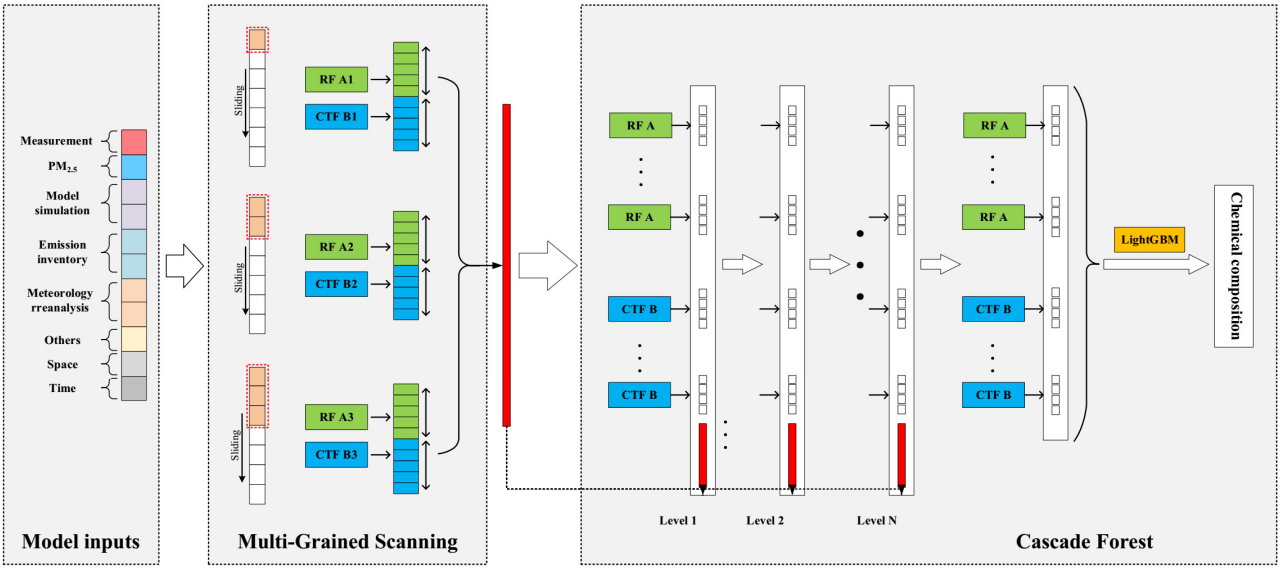

Figure S2. Schematic framework of the four-dimensional spatiotemporal deep forest (4D-STDF) model developed in this study.

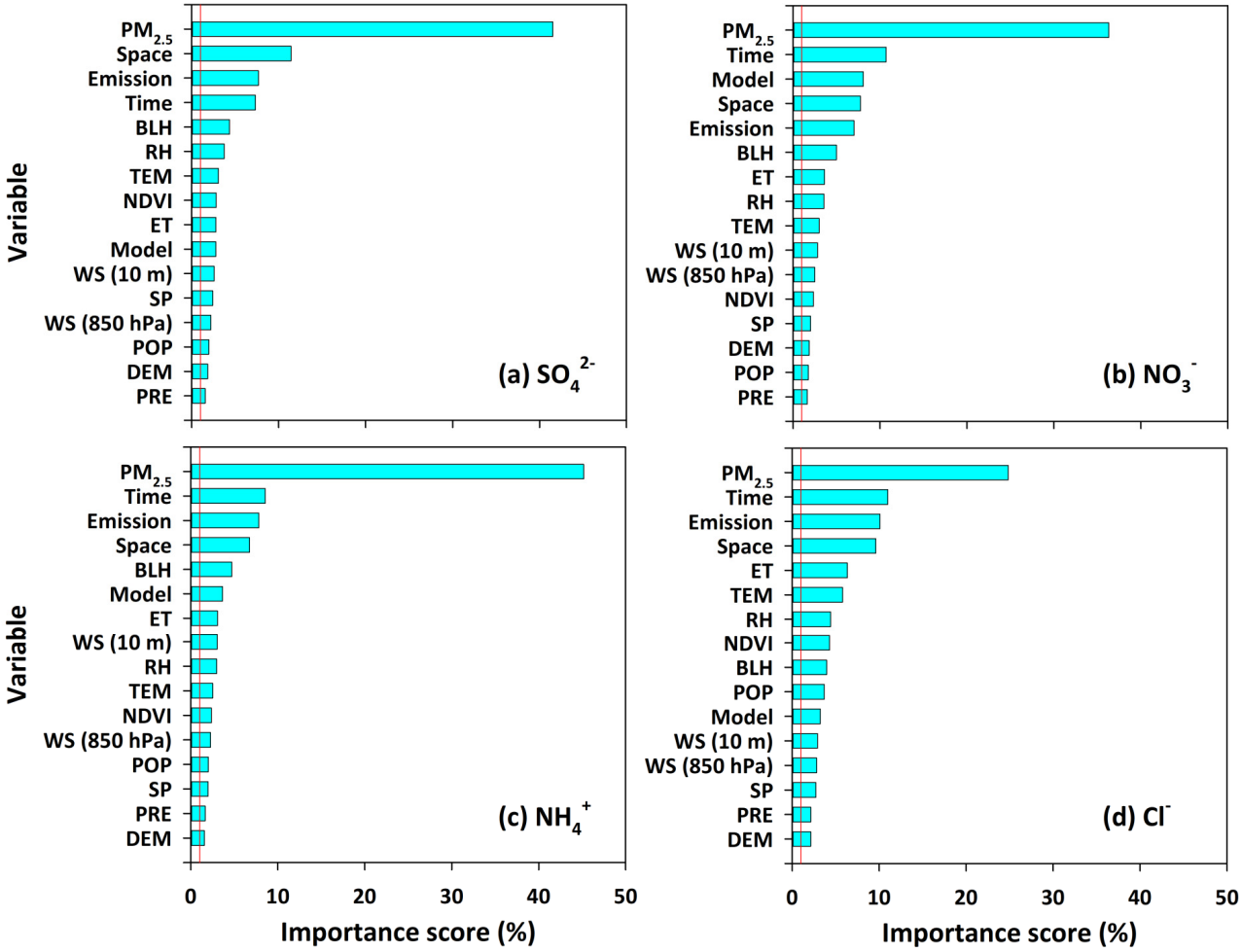

Figure S3. Feature importance for (a) SO_4^{2-}, (b) NO_3^-, (c) NH_4^+, and (d) Cl^- modeling, where the red lines represent the importance score equal to 1%.

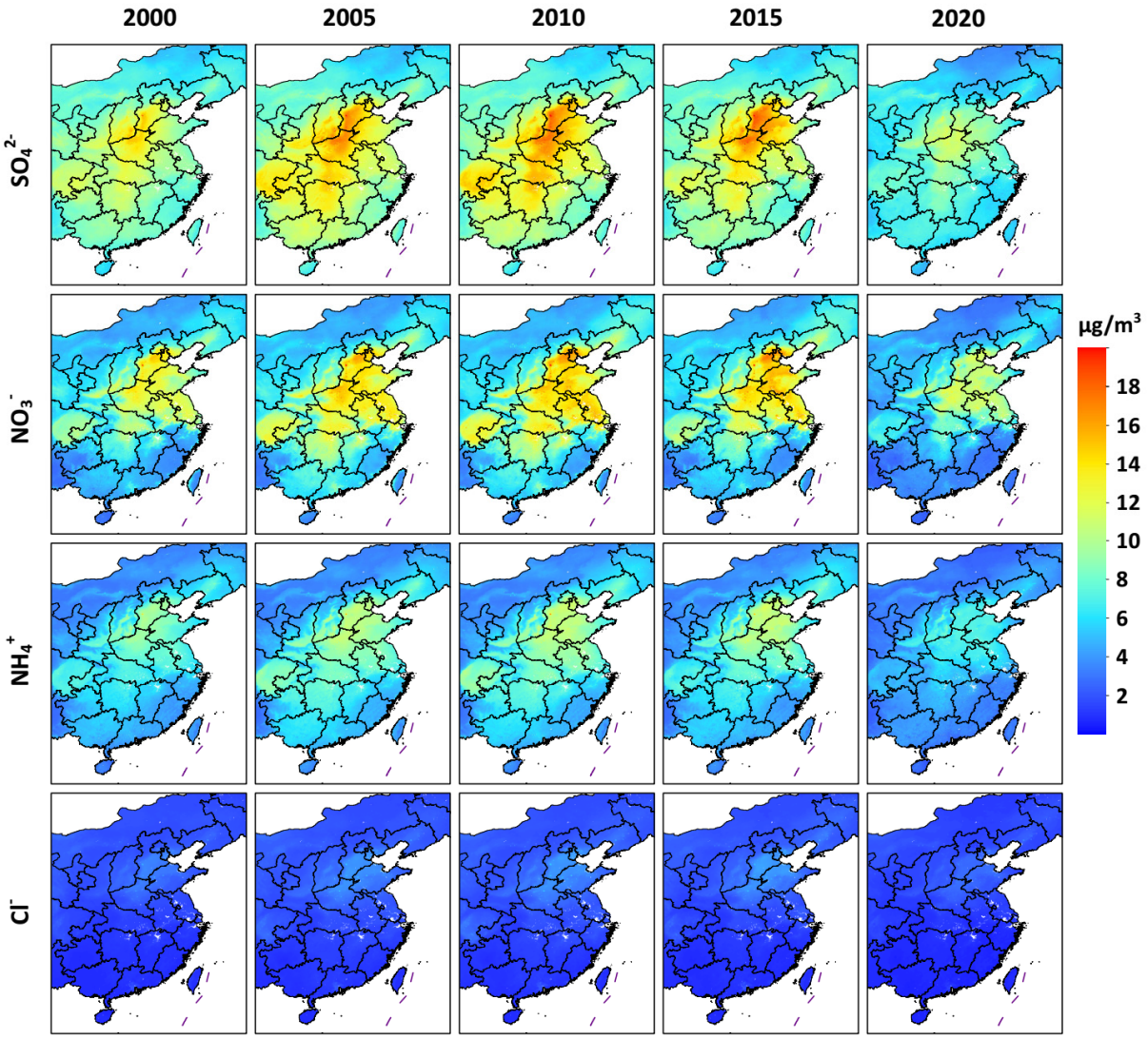

Figure S4. Spatial distributions of annual mean 1-km-resolution of $PM_{2.5}$ inorganic components ($\mu g/m^3$) of SO_4^{2-}, NO_3^-, NH_4^+, and Cl^- in eastern China at an interval of 5 years from 2000 to 2020 in eastern China.

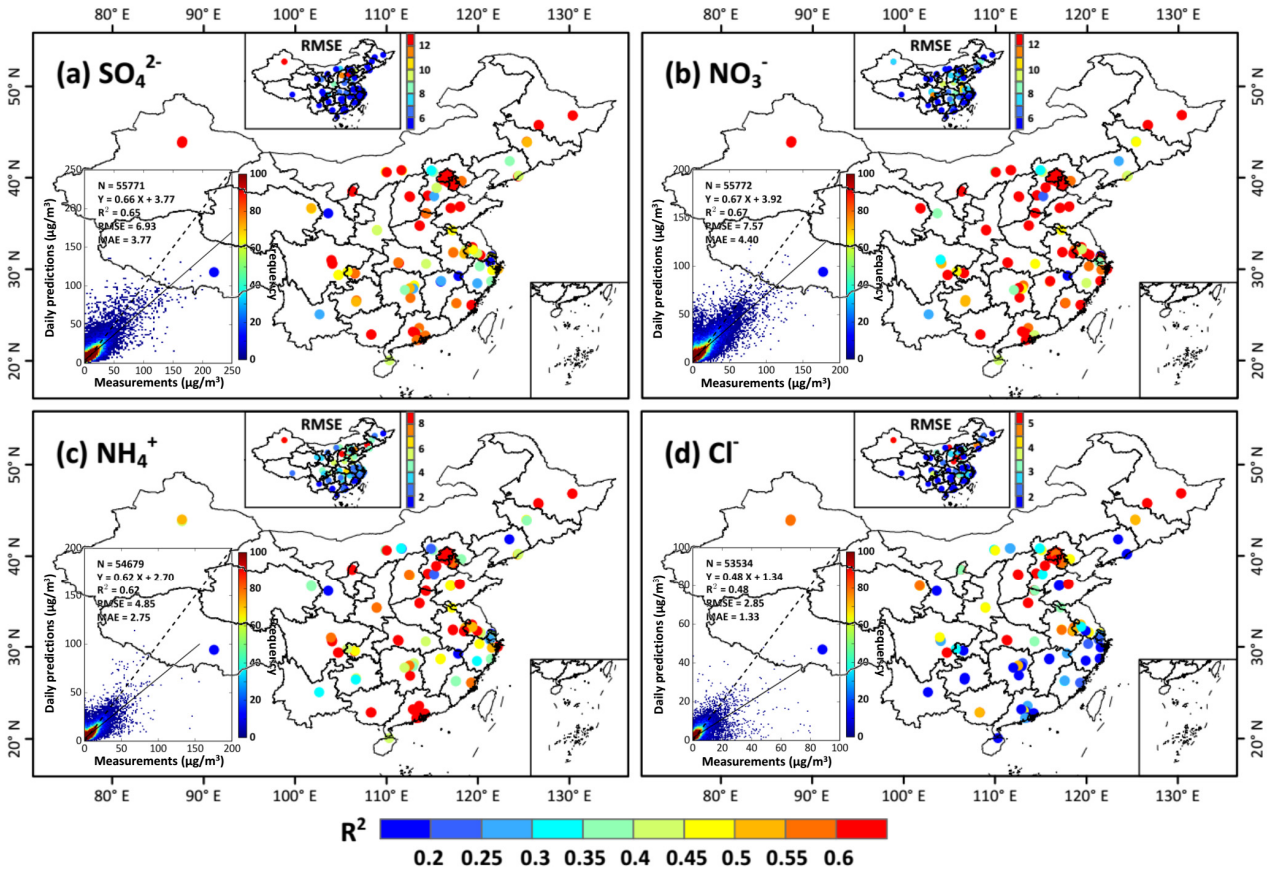

Figure S5. Out-of-station cross validation of daily predictions (μg/m^3) of (a) SO_4^{2-}, (b) NO_3^-, (c) NH_4^+, and (d) Cl^- at each monitoring station and the whole of China (inserted density scatter plots) over the period 2013–2020.

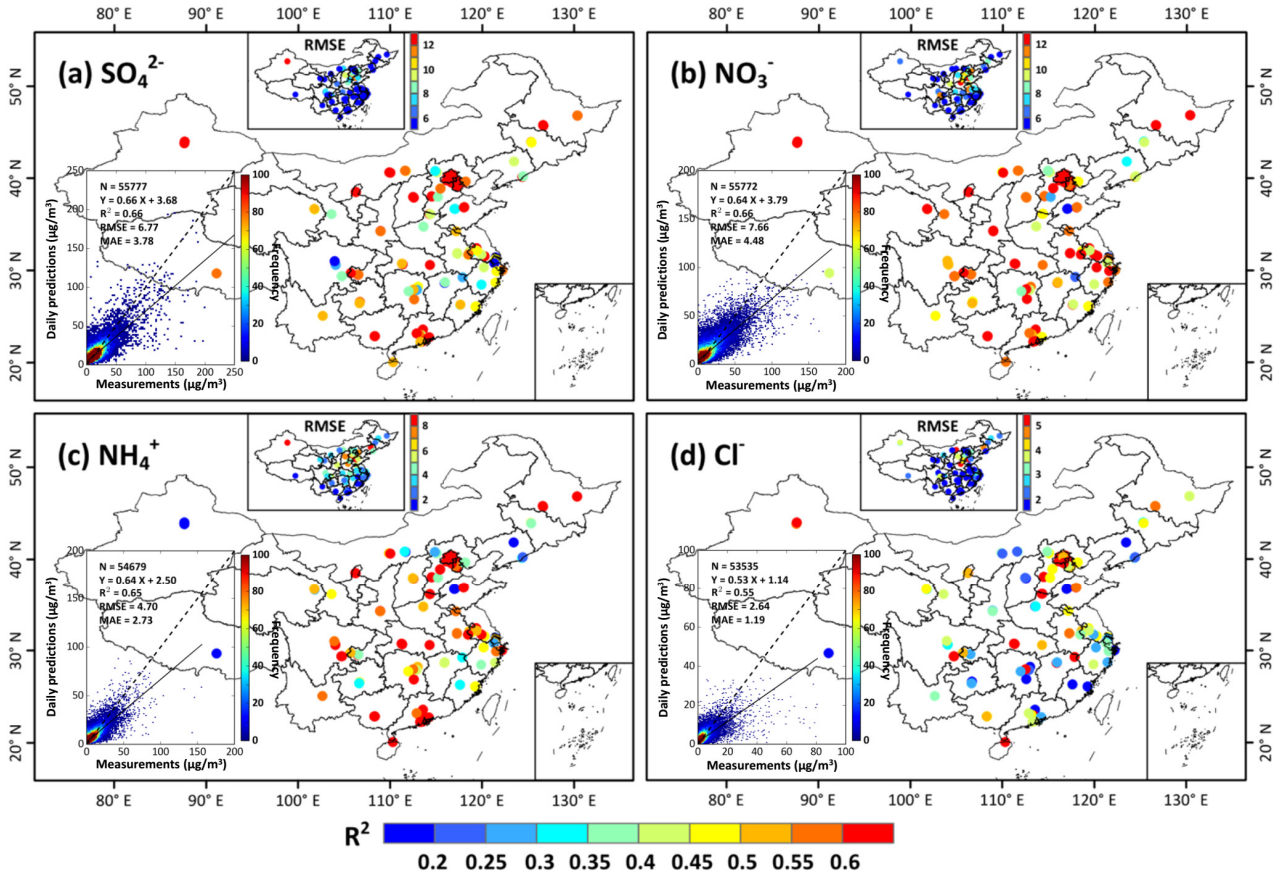

Figure S6. Out-of-day cross validation of daily predictions (μg/m^3) of (a) SO_4^{2-}, (b) NO_3^-, (c) NH_4^+, and (d) Cl^- at each monitoring station and the whole of China (inserted density scatter plots) over the period 2013–2020.

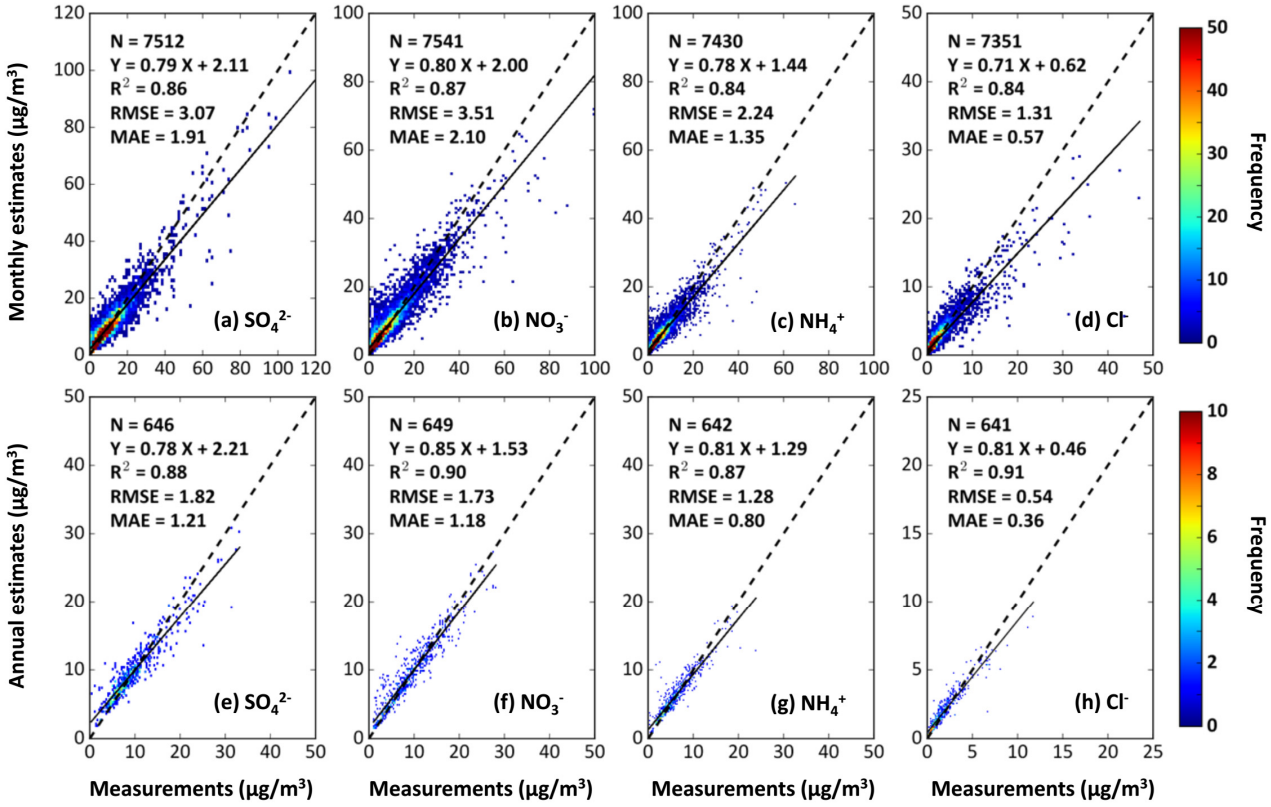

Figure S7. Sample-based validation of (a-d) monthly and (e-h) annual estimates (μg/m^3) of (a) SO_4^{2-}, (b) NO_3^-, (c) NH_4^+, and (d) Cl^- averaged from daily estimates in China over the period 2013–2020.

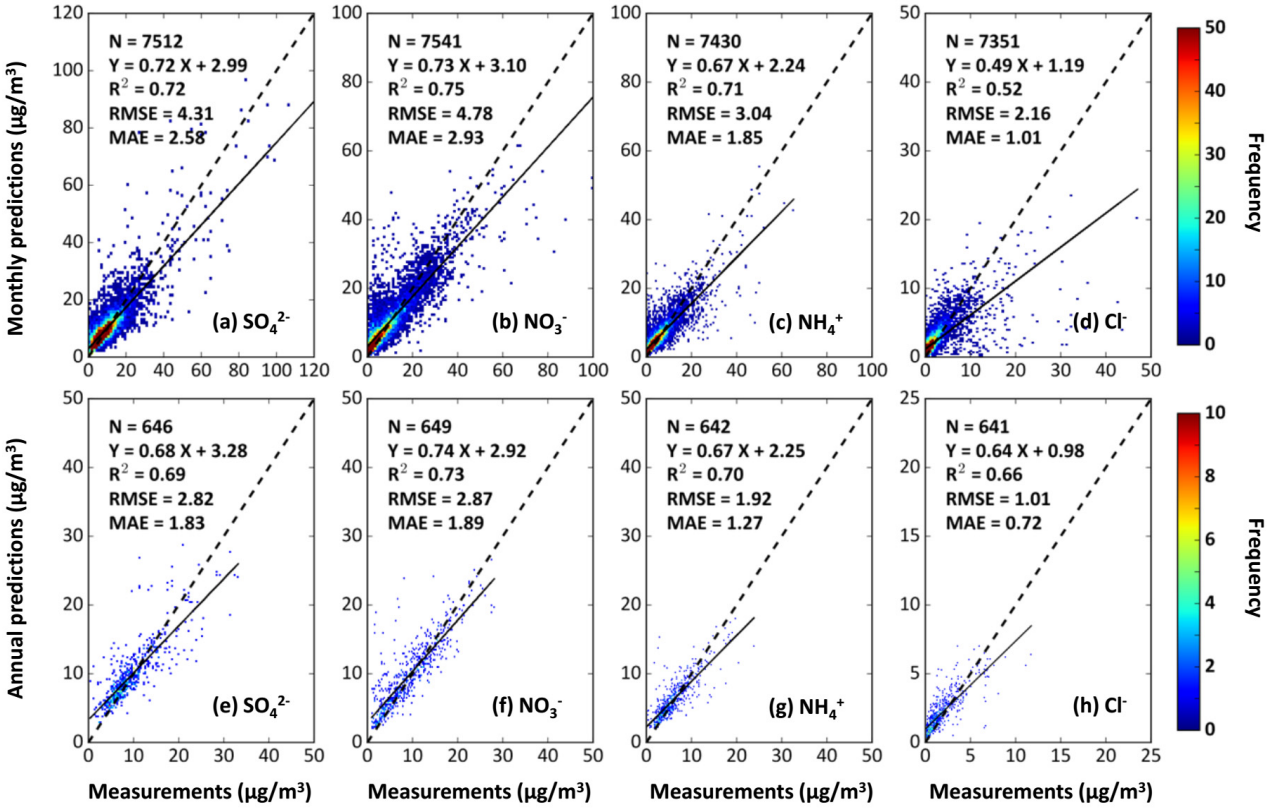

Figure S8. Spatial-based validation of (a-d) monthly and (e-h) annual estimates (μg/m^3) of (a) SO_4^{2-}, (b) NO_3^-, (c) NH_4^+, and (d) Cl^- averaged from daily estimates in China over the period 2013–2020.

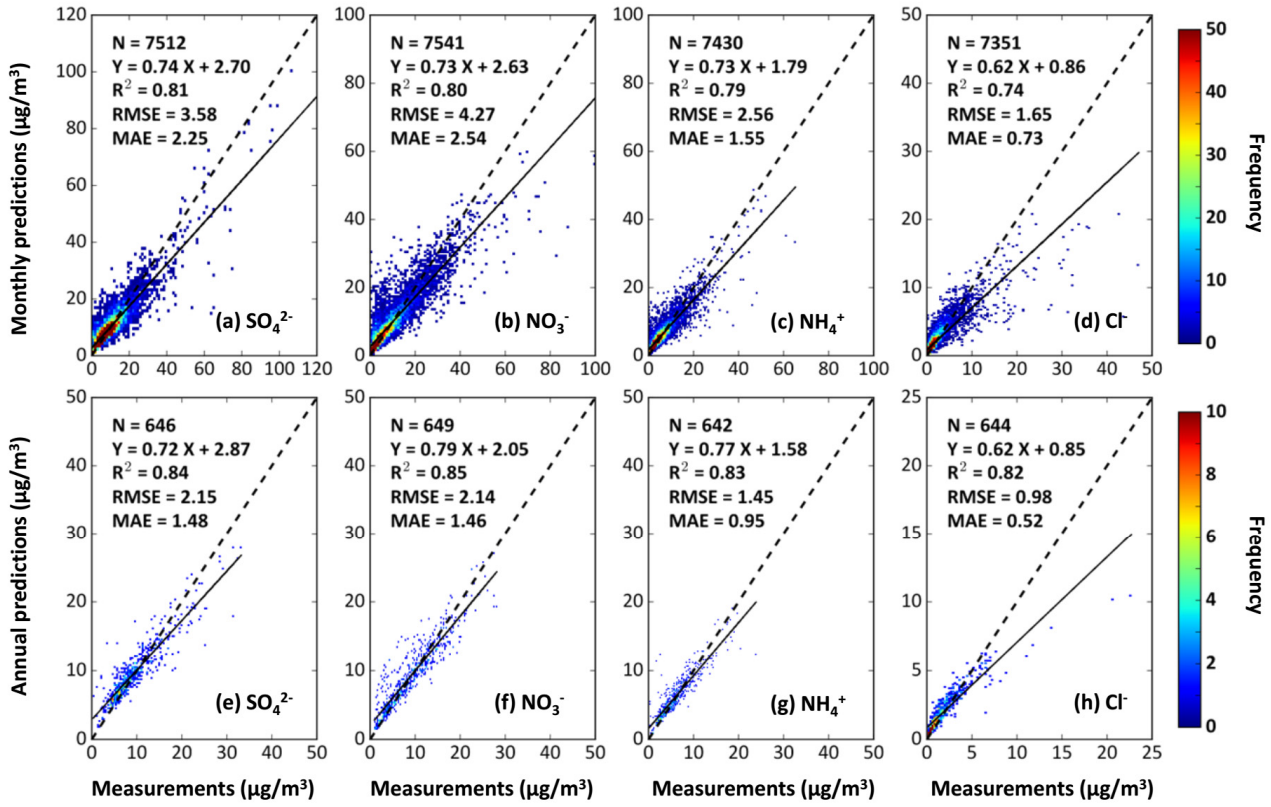

Figure S9. Temporal-based validation of (a-d) monthly and (e-h) annual estimates (μg/m^3) of (a) SO_4^{2-}, (b) NO_3^-, (c) NH_4^+, and (d) Cl^- averaged from daily estimates in China over the period 2013–2020.

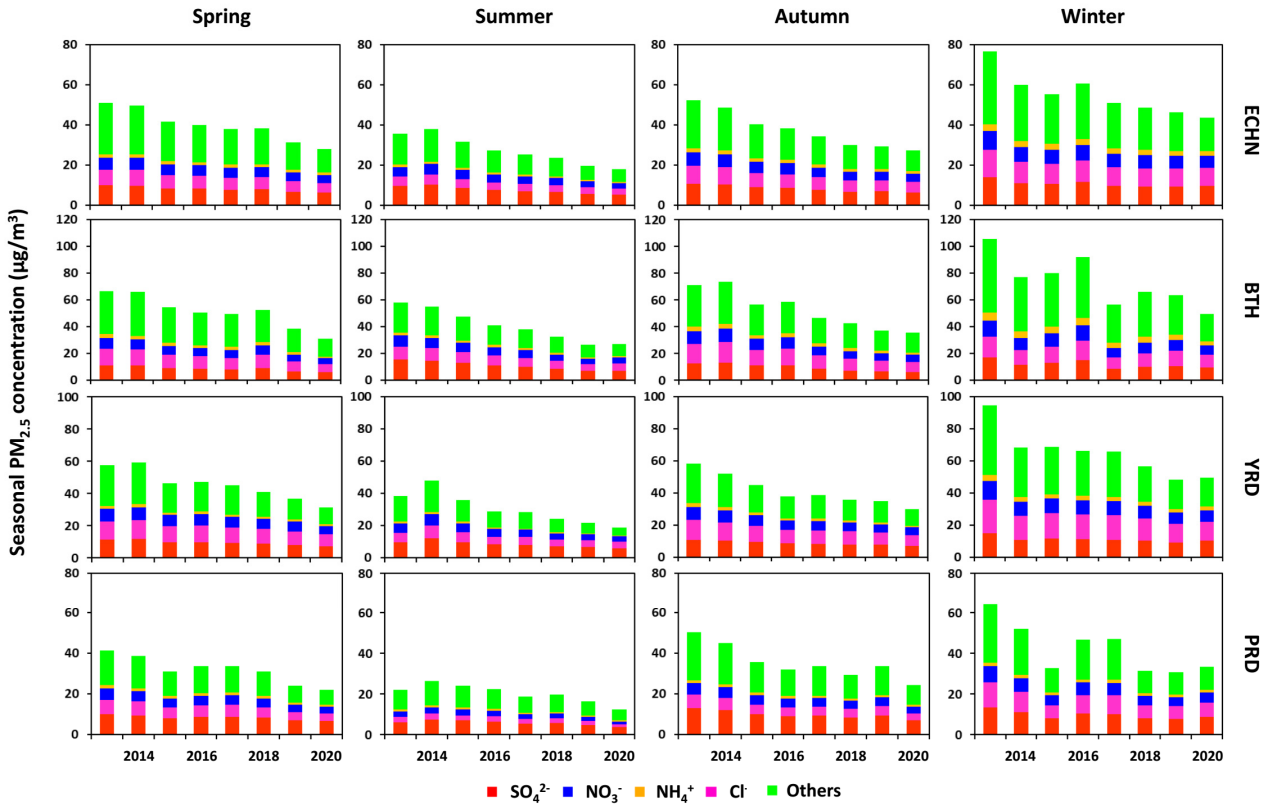

Figure S10. Time series of seasonal population-weighted mean $PM_{2.5}$ concentrations ($\mu g/m^3$) stacked by different chemical components from 2013 to 2020 in (a) eastern China (ECHN), (b) the Beijing-Tianjin-Hebei (BTH) region, (c) Yangtze River Delta (YRD), and (d) Pearl River Delta (PRD), respectively.

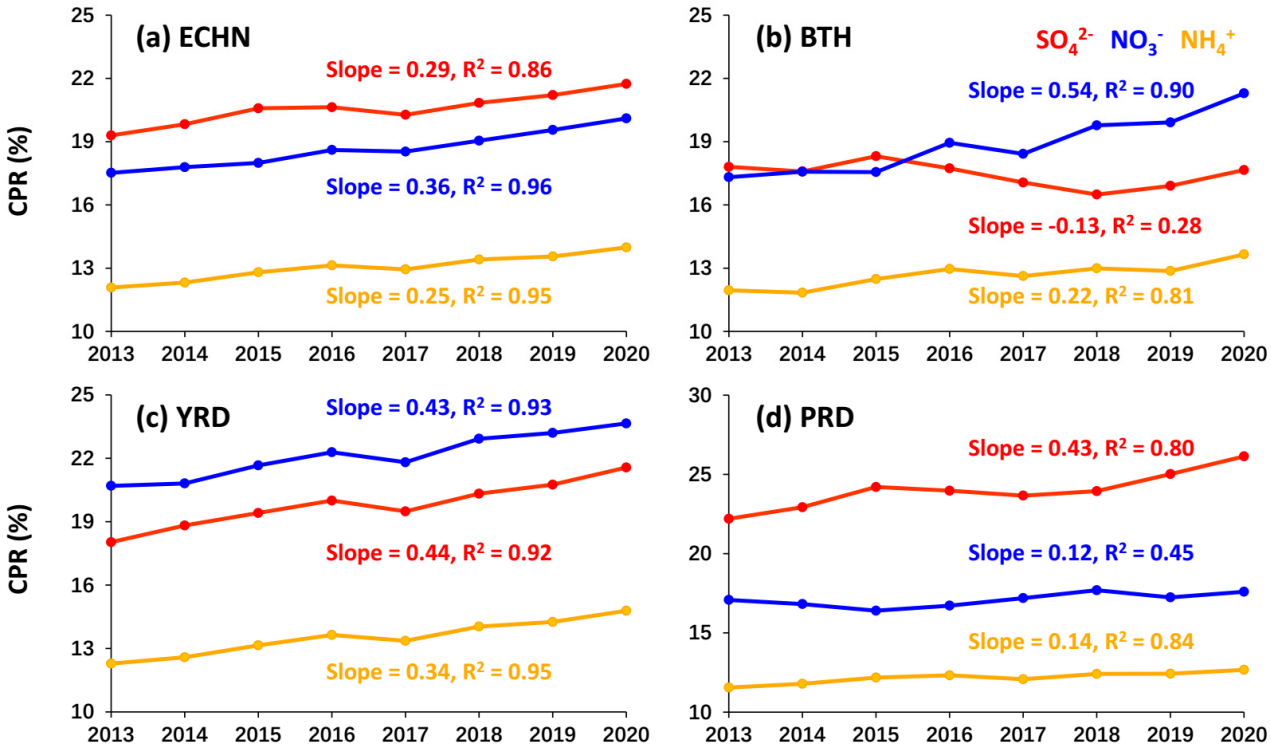

Figure S11. Temporal changes in composition-to-$PM_{2.5}$ ratios (%) of three secondary inorganic aerosols from 2013 to 2020 in (a) eastern China (ECHN), (b) the Beijing-Tianjin-Hebei (BTH) region, (c) Yangtze River Delta (YRD), and (d) Pearl River Delta (PRD), respectively.

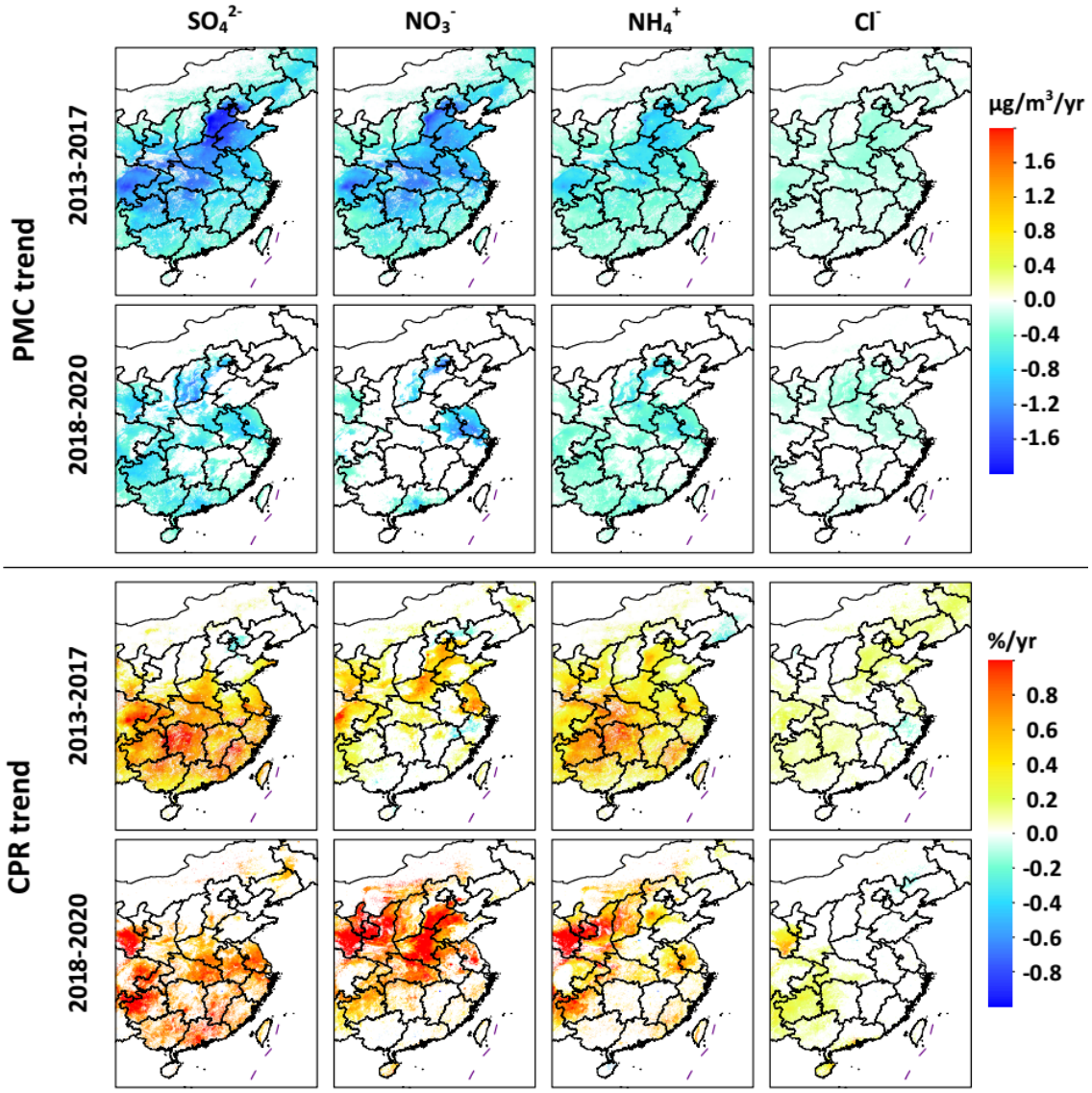

Figure S12. Temporal trends of $PM_{2.5}$ inorganic components (PMC, μg/m^3/yr) and composition-to-$PM_{2.5}$ ratios (CPR, %/yr) of SO_4^{2-}, NO_3^-, NH_4^+, and Cl^- in eastern China during the Clean Air Action Plan (2013–2017) and Blue Sky Defense War (2018–2020). Note that only trends significant at the 95% ($p < 0.05$) confidence level in populated areas (population density > 10 people per km^2) are shown.

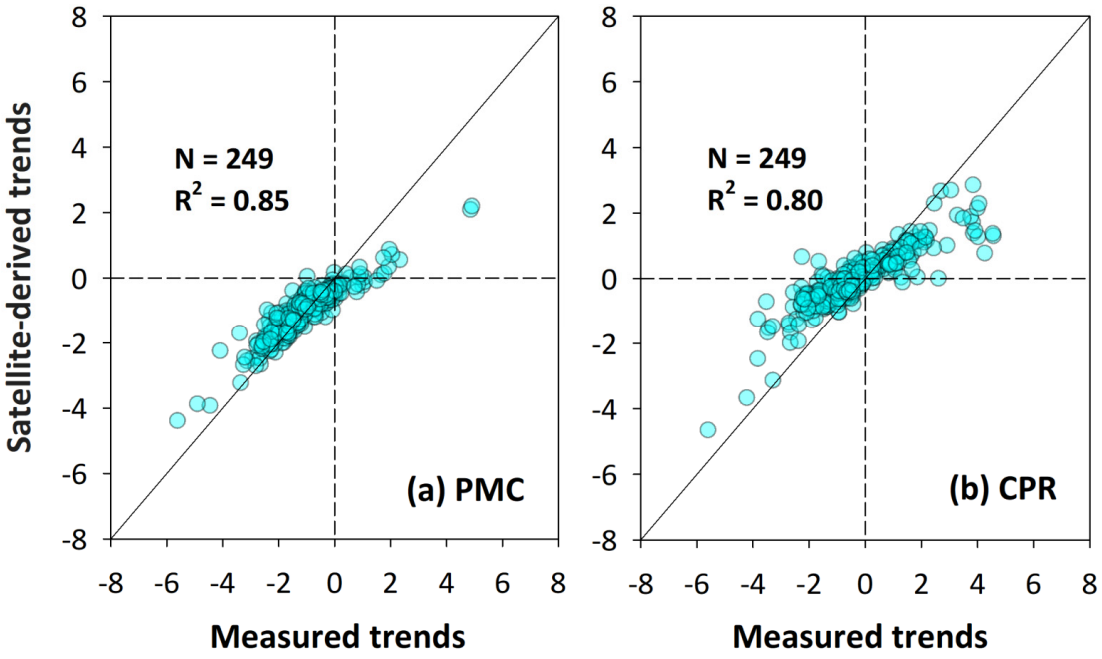

Figure S13. Validation of temporal trends of $PM_{2.5}$ composition (μg/m^3/yr) and composition-to-$PM_{2.5}$ ratios (%/yr) derived from satellite retrievals and ground measurements collocated at all monitoring stations (at least 30% effective observations in a month during the calculation) in China over the period 2013–2020.

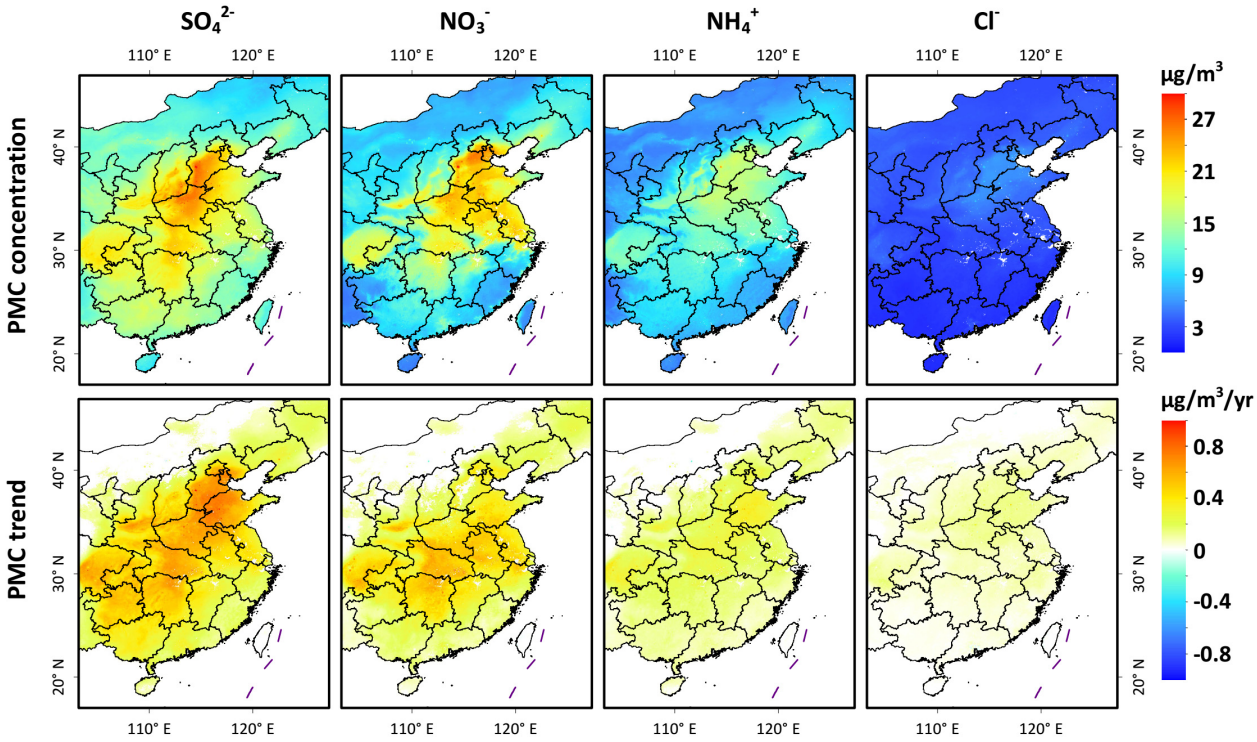

Figure S14. Spatial distributions of multi-year mean concentrations (μg/m^3) and temporal trends (μg/m^3/yr) of $PM_{2.5}$ inorganic components (PMC) of SO_4^{2-}, NO_3^-, NH_4^+, and Cl^- in eastern China during the period 2000–2012.

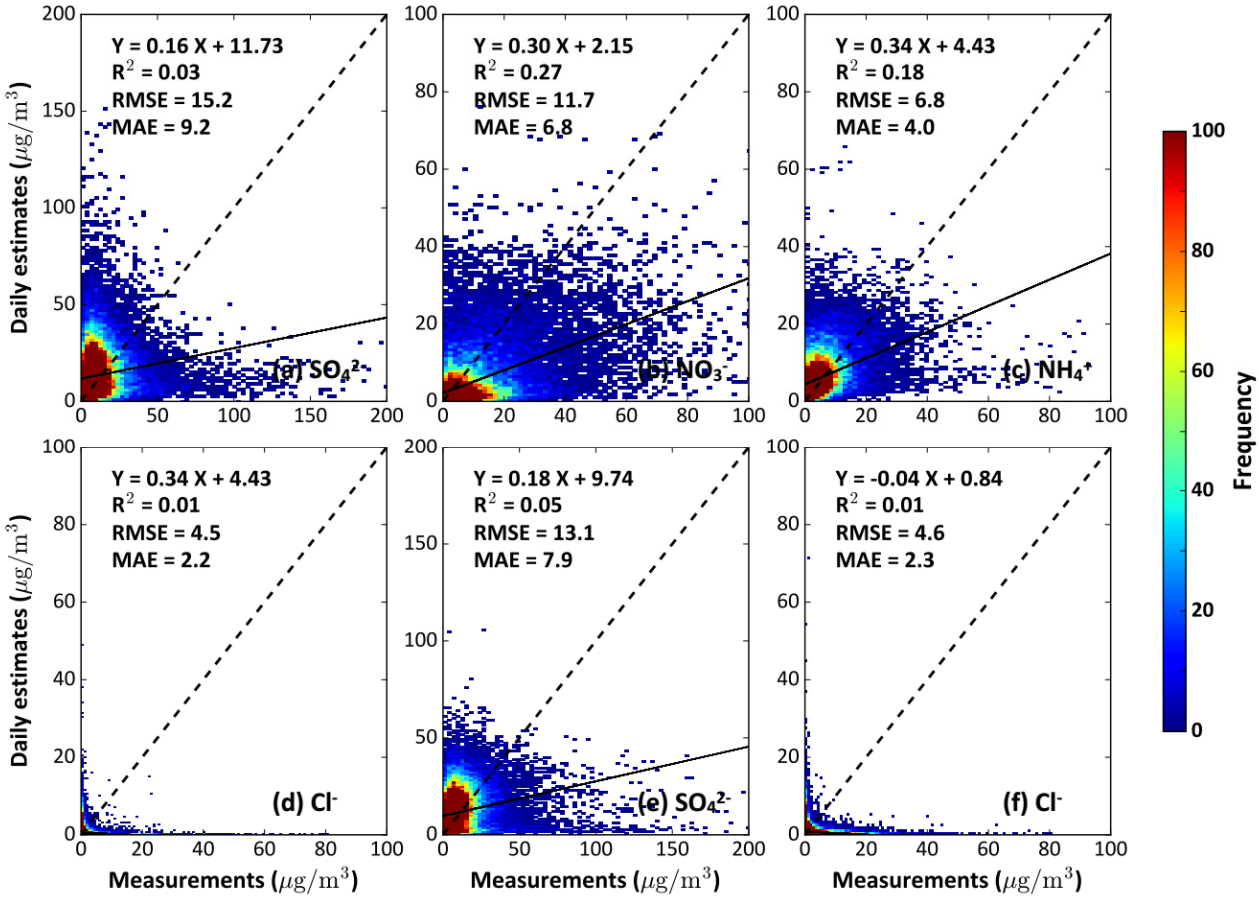

Figure S15. Validation of GEOS-FP daily simulations of (a) SO_4^{2-}, (b) NO_3^-, (c) NH_4^+, and (d) Cl^-, and MERRA2 daily simulations of (e) SO_4^{2-}, and (f) Cl^- against with ground-based measurements in China over the period 2013–2020.

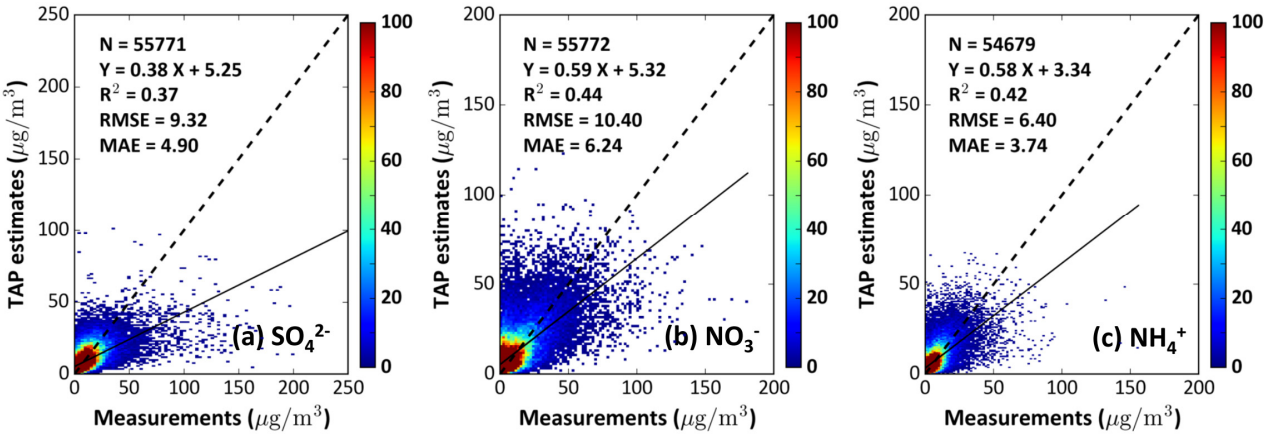

Figure S16. Validation of daily SO_4^{2-}, NO_3^-, and NH_4^+ estimates collected from the Tracking Air Pollution (TAP) in China (http://tapdata.org.cn) against with ground-based measurements from Chinese Center for Disease Control and Prevention network over the period 2013–2020.

Table S1. Summary of the data sources used in this study.

Category	Scientific data set	Unit	Spatial Resolution	Temporal Resolution	Data Source
Ground Measurements	SO_4^{2-}, NO_3^-, NH_4^+, Cl^-	$\mu g/m^3$	Monitor	Daily	CCDCP
	$PM_{2.5}$	$\mu g/m^3$	Monitor	Hourly	MEE
Satellite remote sensing product	Surface $PM_{2.5}$	$\mu g/m^3$	1 km	Daily	ChinHigh$PM_{2.5}$
	Normalized difference vegetation index	-	-	Monthly	MOD13
	Surface elevation	m	90 m	-	SRTM
	Population distribution	people	1 km	Annual	LandScan™
Emission Inventory	Ammonia Nitrogen oxides Sulphur dioxide volatile organic compounds	kg m^{-2} s^{-1}	0.1°×0.1°	Monthly	CAMS
Chemical model simulation	SO_4 surface mass concentration Nitrate surface mass concentration Ammonium surface mass concentration sea salt surface mass concentration	kg m^{-3}	0.3125°× 0.25°	3-hour	GEOS-FP
	SO_4 surface mass concentration sea salt surface mass concentration	kg m^{-3}	0.625°×0.5°	Hourly	MERRA2
Meteorological reanalysis	2-m air temperature	K	0.1°×0.1°	Hourly	ERA5-Land
	Total precipitation	mm			
	Total evaporation	mm			
	10m u-component	m/s			
	10m v-component	m/s			
	Surface pressure	hPa			
	u-component at 850 hPa	m/s	0.25°×0.25°	Hourly	ERA5
	v-component at 850 hPa	m/s			
	Boundary layer height	m			
	Relative humidity	%			

CCDCP: Chinese Center for Disease Control and Prevention; MEE: Chinese Ministry of Environment and Ecology.

Table S2. Statistics of annual and seasonal population-weighted mean $PM_{2.5}$ components (PMC, $\mu g/m^3$) averaged over the period 2013–2020 in eastern China (ECHN), the Beijing-Tianjin-Hebei (BTH) region, Yangtze River Delta (YRD), and Pearl River Delta (PRD), respectively.

ECHN	SO_4^{2-}			NO_3^-			NH_4^+			Cl^-		
	PMC_S	PMC_M	PMC_C	PMC_S	PMC_M	PMC_C	PMC_S	PMC_M	PMC_C	PMC_S	PMC_M	PMC_C
Annual	9.3	10.5	10.6	9.0	10.2	10.6	6.3	6.8	7.0	1.8	2.3	2.4
Spring	8.6	8.9	8.9	8.0	9.3	9.7	5.6	6.2	6.2	1.5	2.0	2.0
Summer	8.1	9.2	9.4	4.4	4.9	5.2	4.1	4.4	4.6	0.9	1.0	1.1
Autumn	8.8	10.2	10.0	8.2	10.3	10.9	5.6	6.8	6.7	1.8	2.2	2.3
Winter	11.1	15.0	14.7	12.4	14.6	15.2	7.9	10.6	10.4	2.9	4.0	4.1
BTH	SO_4^{2-}			NO_3^-			NH_4^+			Cl^-		
	PMC_S	PMC_M	PMC_C	PMC_S	PMC_M	PMC_C	PMC_S	PMC_M	PMC_C	PMC_S	PMC_M	PMC_C
Annual	12.2	12.7	12.8	13.7	14.8	15.3	9.4	9.3	9.7	3.2	3.2	3.4
Spring	9.6	9.3	9.4	12.6	14.7	15.0	7.7	8.4	8.4	2.4	2.5	2.6
Summer	12.9	12.1	12.5	8.6	8.2	8.8	7.1	6.7	7.0	1.5	0.9	1.0
Autumn	11.4	12.0	12.0	15.0	18.7	19.1	8.8	9.6	9.9	3.1	3.1	3.2
Winter	14.0	18.8	19.0	14.8	16.4	17.7	10.8	13.5	13.9	5.5	6.5	6.6
YRD	SO_4^{2-}			NO_3^-			NH_4^+			Cl^-		
	PMC_S	PMC_M	PMC_C	PMC_S	PMC_M	PMC_C	PMC_S	PMC_M	PMC_C	PMC_S	PMC_M	PMC_C
Annual	9.7	8.9	9.1	11.5	11.2	11.7	7.0	6.2	6.4	1.7	1.5	1.5
Spring	9.7	9.4	9.2	10.8	10.6	11.2	6.7	6.4	6.4	1.4	0.9	1.0
Summer	8.7	8.0	8.4	5.7	4.7	5.7	4.6	4.2	4.4	0.8	0.5	0.6
Autumn	8.5	7.2	8.0	9.8	9.3	10.0	5.7	4.6	5.3	1.8	1.7	1.8
Winter	11.1	11.0	11.2	15.9	17.1	17.9	8.8	8.4	8.7	2.7	2.5	2.6
PRD	SO_4^{2-}			NO_3^-			NH_4^+			Cl^-		
	PMC_S	PMC_M	PMC_C	PMC_S	PMC_M	PMC_C	PMC_S	PMC_M	PMC_C	PMC_S	PMC_M	PMC_C
Annual	8.2	8.2	8.1	6.6	5.0	5.3	4.7	3.8	3.9	1.3	0.9	0.9
Spring	8.1	8.5	8.3	6.4	5.5	5.9	4.3	4.1	4.2	1.4	1.1	1.1
Summer	5.6	4.9	5.0	2.3	4.9	2.0	2.2	1.7	1.8	0.7	0.5	0.5
Autumn	9.5	9.5	9.3	5.0	4.1	4.4	4.3	3.8	3.8	1.2	0.7	0.8
Winter	9.2	11.4	10.8	9.3	9.0	9.5	5.6	6.4	6.2	1.7	1.3	1.4

Note: PMC_S, PMC_M, and PMC_C represent the $PM_{2.5}$ components derived from satellites, and measurements and satellites collocated at the same monitoring stations, respectively.

Table S3. Statistics of annual and seasonal composition-to-$PM_{2.5}$ ratios (CPR, %) averaged over the period 2013–2020 in eastern China (ECHN), the Beijing-Tianjin-Hebei (BTH) region, Yangtze River Delta (YRD), and Pearl River Delta (PRD), respectively.

ECHN	SO_4^{2-}			NO_3^-			NH_4^+			Cl^-		
	CPR_S	CPR_M	CPR_C	CPR_S	CPR_M	CPR_C	CPR_S	CPR_M	CPR_C	CPR_S	CPR_M	CPR_C
Annual	20.5	17.7	18.1	19.8	18.1	18.7	13.9	11.7	12.0	3.9	3.7	3.9
Spring	20.1	17.2	17.3	18.7	18.5	19.2	13.0	12.0	12.1	3.4	3.6	3.7
Summer	27.6	26.0	26.8	15.0	14.9	15.7	14.0	12.7	13.1	3.0	2.5	2.8
Autumn	20.9	17.8	17.8	19.5	19.2	19.9	13.2	12.1	12.0	4.2	3.7	4.0
Winter	17.5	16.0	16.0	19.4	16.9	17.5	12.4	11.5	11.5	4.6	4.2	4.5
BTH	SO_4^{2-}			NO_3^-			NH_4^+			Cl^-		
	CPR_S	CPR_M	CPR_C	CPR_S	CPR_M	CPR_C	CPR_S	CPR_M	CPR_C	CPR_S	CPR_M	CPR_C
Annual	17.6	15.6	16.0	19.7	19.9	20.4	13.5	12.0	12.5	4.6	3.9	4.2
Spring	15.5	13.7	14.1	20.3	22.6	23.1	12.4	12.4	12.7	3.9	3.7	3.8
Summer	25.7	24.6	25.6	17.2	18.5	19.5	14.2	14.1	14.7	3.0	1.8	2.1
Autumn	17.1	14.7	15.2	22.6	25.2	25.6	13.2	12.5	13.0	4.7	3.8	4.1
Winter	15.0	14.4	14.9	15.9	14.8	15.6	11.6	11.1	11.5	5.9	5.2	5.4
YRD	SO_4^{2-}			NO_3^-			NH_4^+			Cl^-		
	CPR_S	CPR_M	CPR_C	CPR_S	CPR_M	CPR_C	CPR_S	CPR_M	CPR_C	CPR_S	CPR_M	CPR_C
Annual	19.6	17.9	18.3	23.4	22.8	23.7	14.3	12.5	12.9	3.5	2.7	2.9
Spring	20.0	19.1	19.0	22.4	22.2	23.4	13.9	13.5	13.5	3.0	1.9	2.1
Summer	26.7	25.4	26.4	17.5	15.7	18.1	14.2	13.4	13.9	2.5	1.5	1.8
Autumn	19.7	16.7	18.3	22.7	21.6	22.9	13.3	10.8	12.2	4.2	3.4	3.6
Winter	16.3	14.5	14.7	23.3	23.0	23.8	12.8	11.4	11.7	4.0	3.0	3.3
PRD	SO_4^{2-}			NO_3^-			NH_4^+			Cl^-		
	CPR_S	CPR_M	CPR_C	CPR_S	CPR_M	CPR_C	CPR_S	CPR_M	CPR_C	CPR_S	CPR_M	CPR_C
Annual	23.8	24.3	24.5	19.2	15.5	16.3	13.7	11.6	11.8	3.7	2.6	2.9
Spring	25.1	26.7	26.4	19.8	17.6	18.9	13.4	13.0	13.5	4.3	3.4	3.6
Summer	26.7	25.0	25.7	11.1	10.3	10.5	10.5	8.5	9.0	3.5	2.3	2.6
Autumn	25.4	25.9	25.7	13.3	11.5	12.4	11.5	10.5	10.7	3.3	1.8	2.1
Winter	20.7	21.4	21.2	20.9	18.6	19.5	12.6	12.4	12.4	3.7	2.6	2.9

Note: CPR_S, CPR_M, and CPR_C represent the composition-to- $PM_{2.5}$ ratio derived from satellites, and measurements and satellites collocated at the same monitoring stations, respectively.

Table S4. Statistics of temporal trends in $PM_{2.5}$ components (PMC, μg/m^3/yr) and composition-to-$PM_{2.5}$ ratios (CPR, %/yr) during different periods in Eastern China and key regions.

PMC	2013–2020				2013–2017				2018–2020			
	ECHN	BTH	YRD	PRD	ECHN	BTH	YRD	PRD	ECHN	BTH	YRD	PRD
SO_4^{2-}	-0.63***	-1.06***	-0.65***	-0.53***	-0.72***	-1.11***	-0.78***	-0.54***	-0.41***	-0.57**	-0.51***	-0.72***
NO_3^-	-0.50***	-0.83***	-0.70***	-0.44***	-0.60***	-0.90***	-0.87***	-0.51***	-0.26**	-0.55	-0.60***	-0.55***
NH_4^+	-0.34***	-0.60***	-0.42***	-0.29***	-0.39***	-0.59***	-0.49***	-0.29***	-0.23***	-0.40**	-0.38***	-0.42***
Cl^-	-0.11***	-0.19***	-0.14***	-0.08***	-0.12***	-0.17***	-0.17***	-0.07***	-0.09***	-0.20**	-0.13***	-0.09***
CPR	2013–2020				2013–2017				2018–2020			
	ECHN	BTH	YRD	PRD	ECHN	BTH	YRD	PRD	ECHN	BTH	YRD	PRD
SO_4^{2-}	0.37***	-0.06	0.50***	0.40***	0.34***	-0.04	0.46***	0.33***	0.46***	0.29	0.59***	0.75**
NO_3^-	0.36***	0.57***	0.40***	0.12***	0.28***	0.40***	0.33***	-0.02	0.58***	0.81***	0.50	0.06
NH_4^+	0.26***	0.22***	0.33***	0.09***	0.26***	0.26***	0.31***	0.10**	0.28***	0.26***	0.35***	0.03
Cl^-	0.06***	0.12***	0.02	0.07***	0.06***	0.12***	0.02	0.05	0.05	0.06	0.02	0.28***

Note: ECHN: Eastern China; BTH: Beijing-Tianjin-Hebei; PRD: Pearl River Delta; YRD: Yangtze River Delta.

*: $p < 0.05$; **: $p < 0.01$; ***: $p < 0.001$.

Table S5. Statistics of population-weighted mean $PM_{2.5}$ concentrations ($\mu g/m^3$) and composition-to-$PM_{2.5}$ ratios (%) of SO_4^{2-}, NO_3^-, NH_4^+, and secondary inorganic aerosols (SIA) in heavy haze episodes in the North China Plain over the period 2013–2020.

Date	$PM_{2.5}$ concentration ($\mu g/m^3$)	Composition-to-$PM_{2.5}$ ratio (%)			
		SO_4^{2-}	NO_3^-	NH_4^+	SIA
12/14/2013-12/25/2013	185.7	15.1	14.3	10.4	39.8
01/13/2014-01/20/2014	162.6	16.1	15.5	10.5	42.1
12/19/2015-12/25/2015	186.3	16.1	16.0	11.1	43.2
12/16/2016-12/22/2016	175.8	15.8	17.9	11.7	45.4
01/01/2017-01/09/2017	146.1	17.4	19.4	12.3	49.1
11/24/2018-12/02/2018	132.1	14.5	22.7	12.0	49.2
01/10/2019-01/14/2019	144.1	17.2	20.3	12.4	49.8
01/21/2020-01/26/2020	112.4	16.9	19.4	12.4	48.7
Mean	155.6	16.2	18.2	11.6	45.9

Table S6. Statistics of relative difference (%) population-weighted mean $PM_{2.5}$ components ($\mu g/m^3$) and composition-to-$PM_{2.5}$ ratios (%) of SO_4^{2-}, NO_3^-, NH_4^+, and secondary inorganic aerosols (SIA) during the lockdown period between 2019 and 2020 in Eastern China, three key regions, and Hubei province.

Region	Relative difference in $PM_{2.5}$ components (%)				Relative difference in composition-to-$PM_{2.5}$ ratio (%)			
	SO_4^{2-}	NO_3^-	NH_4^+	SIA	SO_4^{2-}	NO_3^-	NH_4^+	SIA
ECHN	-13.8	-19.7	-16.5	-16.8	7.3	-0.1	3.9	3.5
BTH	5.3	-0.6	3.6	2.4	13.8	7.4	12.0	10.7
YRD	-19.8	-27.2	-22.2	-23.6	7.1	-2.9	3.8	1.9
PRD	-20.3	-16.0	-21.8	-19.1	-4.8	0.5	-6.5	-3.3
Hubei	-27.1	-31.3	-29.6	-29.4	3.7	-2.4	0.1	0.4

Note: ECHN: Eastern China; BTH: Beijing-Tianjin-Hebei; PRD: Pearl River Delta; YRD: Yangtze River Delta.